Separation and Purification Technology 364 (2025) 132550

Contents lists available at ScienceDirect

Separation and Purification Technology

journal homepage: www.elsevier.com/locate/seppur

Effect of pH on the selective electrodialytic recovery of acidogenic-derived volatile fatty acids☆

Kayo Santana Barros [a,b,*], Bruno C. Marreiros [c,d], Manuel César Martí-Calatayud [a], João Goulão Crespo [b,e], Valentín Pérez-Herranz [a], Svetlozar Velizarov [b,*]

[a] IEC Group, ISIRYM, Universitat Politècnica de València – Spain, Camí de Vera s/n, 46022, P.O. Box 22012, València E-46071, Spain
[b] LAQV/REQUIMTE, Department of Chemistry, NOVA School of Science and Technology, NOVA FCT, Universidade NOVA de Lisboa, 2829-516 Caparica, Portugal
[c] Associate Laboratory i4HB - Institute for Health and Bioeconomy, NOVA School of Science and Technology, Universidade NOVA de Lisboa, 2829-516 Caparica, Portugal
[d] UCIBIO – Applied Molecular Biosciences Unit, Department of Chemistry, NOVA School of Science and Technology, Universidade NOVA de Lisboa, 2829-516 Caparica, Portugal
[e] ITQB, Universidade NOVA de Lisboa, Av. da República, 2780-157 Oeiras, Portugal

ARTICLE INFO

Editor: Dr. B. Van der Bruggen

Keywords:
polyhydroxyalkanoate (PHA)
PHA precursors
Biobased plastics
VFAs fractionation
Chronopotentiometry

ABSTRACT

Electrodialysis can be utilized to separate acidogenic-derived volatile fatty acids (VFA) used in the production of biobased and biodegradable polyhydroxyalkanoates (PHA). All VFAs are commonly recovered simultaneously in the receiver solution, although their selective recovery could benefit the fermentation process. The effect of membrane type, electric voltage and time on this selective recovery has been studied, but the impact of solution pH — an essential factor in organic acids separation — remains still not sufficiently explored. Herein, the effect of the initial feed pH on the fractionation degree of four VFAs commonly present in fermented solutions — namely acetic, propionic, butyric, and valeric acid — was systematically evaluated. Three distinct anion-exchange membranes were tested: Ralex AMH-PES, Fumasep FAS-PET-130, and PC200D. It was found that pH significantly influenced VFA separation with the PC200D membrane, particularly enhancing the transfer of smaller organic anions, such as acetate and propionate, while the percent extraction (PE%) of larger anions, such as butyrate and valerate, remained practically unchanged as the pH increased. Thus, the higher the pH, the greater the fractionation degree achieved. For the electrodialysis operated with a feed solution at pH 7, ratios of $(PE_{Ac} + PE_{Prop})/(PE_{But} + PE_{Val})$ and PE_{Ac}/PE_{Val} of 1.6 and 2.0, respectively, were obtained. This may be related to the presence of tertiary amines in the PC200D's fixed groups, which enhanced water dissociation occurrence. The transfer of VFAs through the Ralex and Fumasep membranes was less affected by pH as they contain only quaternary ammonium as their fixed charged groups.

1. Introduction

Polyhydroxyalkanoates (PHA) are biobased, biocompatible, and biodegradable polymers synthesized by microorganisms primarily serving as carbon and energy storage materials. PHAs are recognized as a sustainable alternative to traditional plastics across various sectors due to their diverse physicochemical characteristics, which are determined by the composition and arrangement of their monomeric units [1,2]. Consequently, PHAs are classified based on their monomeric composition: short-chain-length PHAs (scl-PHAs) contain 3 to 5 carbon units, medium-chain-length PHAs (mcl-PHAs) have 6 to 14 carbon units, and long-chain-length PHAs (lcl-PHAs) consist of more than 14 carbon units [1,2].

In the production of PHAs using mixed microbial cultures (MMCs), acetic, propionic, butyric, and valeric acids are the most frequently utilized precursor molecules. This is because these compounds, collectively known as volatile fatty acids (VFA), are primarily produced during the acidogenic fermentation of complex organic substrates, such as industrial by-products or waste streams [3].

The VFA profile of the fermented solution supplied to the MMC

☆ This article is part of a special issue entitled: 'In Honor of Prof De Pinho' published in Separation and Purification Technology.

* Corresponding authors at: LAQV/REQUIMTE, Department of Chemistry, NOVA School of Science and Technology, NOVA FCT, Universidade NOVA de Lisboa, 2829-516 Caparica, Portugal.
E-mail addresses: kasanbar@alumni.upv.es (K.S. Barros), s.velizarov@fct.unl.pt (S. Velizarov).

https://doi.org/10.1016/j.seppur.2025.132550
Received 2 February 2025; Received in revised form 12 March 2025; Accepted 14 March 2025
Available online 15 March 2025

during PHA production is crucial, as it significantly influences both the composition of the resulting PHAs and their properties, as well as the overall production yield. In particular, during the synthesis of scl-PHAs, 3-hydroxyvalerate (3HV) monomers can be derived from either a single molecule of valeric acid or from an equal combination of acetic and propionic acids. Similarly, 3-hydroxybutyrate (3HB) monomers can originate from either one molecule of butyric acid or from two molecules of acetic acid. Additionally, the synthesis of PHAs from each mole of VFA requires two moles of ATP, meaning one mole for active transport and another for intracellular conversion. As a result, VFAs with longer carbon chains, such as butyric and valeric acids, demand less ATP for the production of one C-mol of PHA compared to shorter-chain VFA like acetic and propionic acids [4].

Enhancing control over the composition of VFA in the fermented streams provided to MMCs during PHA production can lead to reductions in overall production costs and improve the precision of the desired monomer composition and consistency of the produced PHAs. To address the aforementioned challenges, an effective strategy could involve the recovery and separation of VFAs from the commonly used fermented solutions in MMC processes, thereby allowing for the targeted selection of specific types of VFAs introduced to the culture during PHA accumulation.

In recent years, membrane separation techniques have been frequently employed to extract nutrients (mainly nitrogen) or VFAs from the fermented solution, such as forward osmosis [5], membrane extraction [6], Donnan dialysis, [7,8] and electrodialysis [9,10]. Recently, the use of electrodialysis (ED) for recovering VFAs derived from PHA production was systematically evaluated [10]. The influence of the type of anion-exchange membrane (AEM), electric voltage, and operating time on the selectivity degree of VFAs separation was assessed. However, the impact of the pH of the fermented solution was not evaluated, although this is an operational parameter that significantly influences the transport of organic acids through AEMs. Several authors have shown that pH affects the chemical equilibrium of species in both the bulk solution and the membrane surface, altering the type and mobility of the species being transferred through the membrane [11,12]. In addition to the initial pH affecting the ED performance, the feed solution pH varies over time due to the dynamic transport of species through the membranes. Besides, the membrane/solution system is also subject to significant pH changes caused by water dissociation at the membrane surface and the resulting formation of H^+ and OH^- ions [13]. Therefore, it is crucial to evaluate the influence of the solution pH on the percent extraction and selectivity degrees of species especially when working with complex solutions such as fermented ones.

In addition to evaluating ED performance, it is essential to assess the transport mechanisms and fouling/sorption phenomena occurring at the membrane under different operational conditions, since fouling is one of the major limitations of electrodialysis [14,15]. Chronopotentiometry can be used for this purpose, which is a helpful technique that allows for evaluating the evolution of the potential drop of the membrane/solution system over time. The chronopotentiograms (ChPs) provide valuable information on the dominant ion transport mechanisms through the membrane, such as diffusion/migration, gravitational convection and electroconvection, in addition to water dissociation phenomenon [11,16].

In this study, the influence of solution pH on the selective recovery, by electrodialysis, of VFAs commonly present in biomass fermentation for PHA production was evaluated. Feed solutions containing acetic, propionic, butyric and valeric acids at different initial pH values (from 3 to 7) and three commercial AEMs with distinct characteristics (namely, Ralex AMH-PES, Fumasep FAS-PET-130, and PC200D) were tested. The mechanisms of ion transfer through the membranes were assessed using chronopotentiometry.

2. Materials and Methods

2.1. Electrodialysis and chronopotentiometry cell

The ED and chronopotentiometry experiments were conducted using a commercial ED-Z mini unit (Mega, Czech Republic) presenting four compartments with an AEM at the center and a cation-exchange membrane (CEM) at the ends of the cell, as represented in Fig. 1. The effective area of the membranes was 64 cm^2. A platinum wire was placed at each side of the AEM for the chronopotentiometry experiments. Spacers with transverse filaments were placed at both surfaces of the CEMs to enhance turbulence, while spacers without filaments were placed at both surfaces of the AEM to increase the distance between the platinum wires and the spacer filaments. In the ED experiments, the two compartments adjacent to the AEM contained the feed and receiver solutions, respectively, while the two end compartments contained the electrode rinse solution. The feed consisted of a solution initially containing the VFAs, the receiver was composed of a NaCl solution, and a Na_2SO_4 solution flowed through the electrode compartments. The feed and receiver compartments were connected to external reservoirs containing 250 ml of their respective solutions in the ED tests and 500 ml in the chronopotentiometry tests, whereas the electrode compartments were connected to the same reservoir containing 500 ml of the electrode solution in both ED and chronopotentiometry tests. The solutions circulated through the cell and reservoirs at a flow rate of 13.2 L/h. The solutions in the reservoirs were stirred by a magnetic stirrer. The anode and cathode electrodes were connected to a potentiostat/galvanostat (Autolab PGSTAT204, Utrecht, The Netherlands), which supplied the electric voltage/current. In the chronopotentiometry experiments, the sensing and reference cables of the potentiostat were connected to the platinum wires. The experiments were conducted at room temperature, in duplicate, and the estimated relative errors between the results were below 5 %.

2.2. Chronopotentiometry procedure

The chronopotentiometry experiments were conducted using the ED cell shown in Fig. 1 but using the same solution in the feed and receiver reservoirs. Feed solutions with initial pH values of 5, 6 and 7 were tested. Several experiments were performed under increasing current density values. Each experiment was conducted in two steps: (1) measurement of the potential drop of the membrane/solution system (E_m)

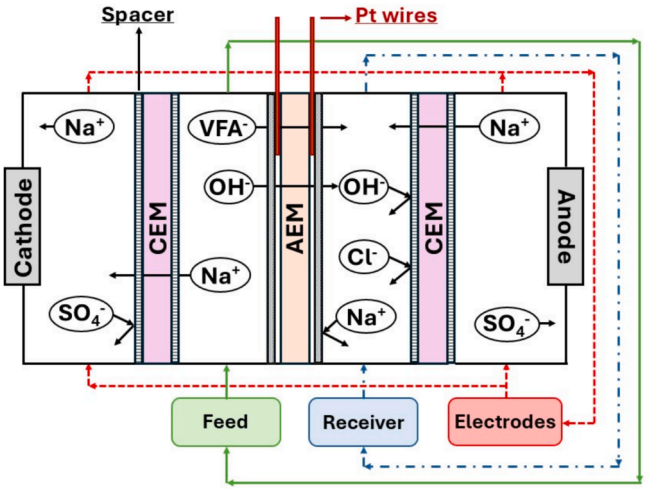

Fig. 1. Schematic representation of the electrodialysis and chronopotentiometry cell. The solid, dash-dotted, and dashed lines connect the feed, receiver and electrodes rinse solution compartments to their respective reservoirs.

for 400 s under the application of electric current, and (2) measurement of E_m for 200 s during system relaxation without applying electric current. The current values applied in step (1) were based on a recent study conducted with feed solutions at pH 6 and an ED system identical to the one used here. In the previous study, the current density values were defined based on linear sweep voltammetry (LSV) curves of the membrane/solution systems [10].

Current-voltage curves (CVC) of each membrane/solution system were constructed from the applied current densities and the respective E_m values measured immediately before the interruption of current application in step (1), as represented in Fig. S1 of the Supplementary Material. The limiting current density (i_{lim}), ohmic resistance (R_{ohm}), and overlimiting resistance (R_3) were determined from the obtained CVCs. i_{lim} was obtained by determining the intersection of the tangent lines of the first (quasi-ohmic) and second (plateau) regions of the CVC. R_{ohm} was determined by calculating the inverse of the slope (α_1) of the tangent line of the quasi-ohmic region, while R_3 was determined similarly, but considering the slope (α_3) of the tangent of the third (overlimiting) region [17].

2.3. Electrodialysis operation

The ED experiments were conducted using feed solutions at initial pH values of 3, 4, 5, 6 and 7, in potentiostatic mode under 2.35 V. This voltage value was chosen based on a recently published study, which demonstrated that it provides the optimal trade-off between percent extraction and degree of fractionation of the VFAs using a feed solution at pH 6 and the same ED cell used herein [10]. Before each experiment, deionized water was circulated through the cell and reservoirs to remove residues of VFAs from the previous experiment. Then, the feed, receiver and electrodes reservoirs were filled with their respective solutions, the pumps were turned on, and the voltage was applied after approximately 1 min of circulation of the working solutions. The duration of the ED experiments was 3 h. Samples of 3 mL were withdrawn throughout the experiments (at 0 h, 0.5 h, 1 h, 2 h and 3 h) from the feed and receiver reservoirs, respectively, for analyzing VFAs concentration and pH. [10].

Before conducting the tests, a LSV curve of the ED stack (electrodes) was constructed to evaluate the relationship between applied voltage and current density of the cell. The AEM used in the LSV construction was Fumasep, and the feed solution had a pH of 6. The LSV parameters were as follows: scan rate of 0.002 V/s, step of 0.01 V, and final potential of 3 V.

2.3.1. Analytical methods

The concentration of VFAs in the samples withdrawn were analyzed via high-performance liquid chromatography (HPLC) using a VWR Hitachi Chromaster system (Hitachi, Tokyo, Japan). This setup included a Pump 5160, an auto-sampler 5260, a Column Oven 5310, a Diode Array Detector 5430, a Refractive Index (RI) Detector 5450, a Biorad 125–0129 30 × 4.6 mm pre-column, and an Aminex HPX-87H 300 × 7.8 mm column. The elution was performed with 0.01 mol/L H_2SO_4 at a flow rate of 0.6 mL/min and a column temperature of 60 °C. pH measurements of the solutions were carried out using a Sension +pH3 meter (Hach, Loveland, CO, USA).

2.4. Ion-exchange membranes

The ED and chronopotentiometry experiments were conducted using three commercial AEMs (Ralex AMH-PES, Fumasep FAS-PET-130, and PC200D) that exhibit distinct characteristics, particularly in terms of heterogeneity, thickness, and type of functional groups. The two CEMs present at the two ends of the cell were of the Ralex CMH-PES type. The main characteristics of the membranes used are shown in Table S1 (see the Supplementary Material).

The Ralex membrane is heterogeneous and thicker, while the Fumasep and PC200D membranes are homogeneous and significantly thinner. The functional group of the Ralex and Fumasep membranes is quaternary ammonium, whereas the PC200D membrane contains both tertiary amines and quaternary ammonium groups.

2.5. Solutions

All solutions were prepared with deionized water. The feed solution was prepared with the following VFAs: acetic acid (Fisher Scientific, Loughborough, UK), propionic acid, butyric acid, and valeric acid (Acros Organics, Geel, Belgium). Each VFA was present at an equimolar concentration of 25 mmol/L, which was defined based on real fermented solutions and to eliminate ion transport effects due to concentration differences [7,10]. NaOH (Fisher Scientific, Loughborough, UK) was used for pH adjustment. The pH range was chosen based on the pH of real feed solutions [18].

The receiver solution was 0.1 mol/L NaCl and the electrode rinse solution 0.14 mol/L (20 g/L) Na_2SO_4 (Panreac, Barcelona, Spain).

2.6. Equations

The performance of ED was evaluated by calculating the percent extraction (PE%) of VFAs from the feed solution using Equation (1). In this equation, C_F^j is the concentration of a given VFA (j) in the feed (F) compartment at the beginning ($t = 0$) and at a given time ($t = i$) when samples were withdrawn.

$$PE\% = \left(1 - \frac{C^j_{F(t=i)}}{C^j_{F(t=0)}}\right) \bullet 100 \quad (1)$$

With the PE% results, the ratios of PE% for the following VFAs were calculated: acetic/(butyric + valeric) ($PE_{Ac}/(PE_{But} + PE_{Val})$), propionic/(butyric + valeric) ($PE_{Prop}/(PE_{But} + PE_{Val})$), (acetic + propionic)/(butyric + valeric) ($PE_{Ac} + PE_{Prop})/(PE_{But} + PE_{Val}$) and acetic/valeric ($PE_{Ac}/PE_{Val}$). These ratios were calculated to evaluate the degree of fractionation in the separation of the VFAs: the higher the ratio, the greater the difference between the PE% values, indicating more effective fractionation. The first two ratios reflect the separation of the smallest VFAs (acetic or propionic) from the largest ones (butyric and valeric) evaluated here, while the third ratio reflects the simultaneous separation of the smallest VFAs (acetic and propionic) from the largest ones. The latter ratio reflects the separation of the smallest (acetic) and largest (valeric) VFAs. Among the ratios evaluated here, the most relevant is $(PE_{Ac} + PE_{Prop})/(PE_{But} + PE_{Val})$, as the aim of the study is to assess the separation of acetic and propionic acids from butyric and valeric acids.

With concentration data of the VFAs, the deviation of the total number of moles of each VFA present in the solutions relative to the theoretical number of moles, which corresponds to the initial value, was calculated (mass balance) for each time (i) using Eqs. (2) – (4). In these equations, the moles of each VFA (j) in the feed (F) and receiver (R) compartments, as well as in the samples at the initial time ($t = 0$) and at each sampling time ($t = i$), was considered. In the equations, C and V refer to the VFA molar concentration and reservoir volume, respectively. The reservoir volume considered in the equations is theoretical and was determined by subtracting the volume of the aliquots withdrawn from each compartment throughout the experiment.

$$Mass\ balance\%_{(t=i)} = \left(\frac{VFA^j moles_{(F+R+aliquots)\,(t=i)}}{VFA^j moles_{(F+R)\,(t=0)}}\right) \bullet 100 \quad (2)$$

$$VFA^j moles_{(F+R)\,(t=0)} = C^j_{F(t=0)} V_{F_{(t=0)}} + C^j_{R(t=0)} V_{R_{(t=0)}} \quad (3)$$

$$VFA^{j}moles_{(F+R+aliquots)_{(t=i)}} = \left(C^{j}_{F(t=i)} \times V_{F_{(t=i)}}\right) + \left(C^{j}_{R(t=i)} \times V_{R_{(t=i)}}\right) + \sum_{i=0}^{i}\left[C_{(aliquotsofF)_{(t=i)}} \times V_{(aliquotsofF)_{(t=i)}}\right] + \sum_{i=0}^{i}\left[C_{(aliquotsofR)_{(t=i)}} \times V_{(aliquotsofR)_{(t=i)}}\right] \quad (4)$$

3. Results and Discussion

The speciation diagram of the aqueous solution containing the four VFAs evaluated in the present study is shown in Fig. S2 of the Supplementary Material. All the VFAs are monoprotic, and the following pKa values were used for the construction of the curves: acetic (4.76), propionic (4.87), butyric (4.83) and valeric (4.82) acids [19,20]. As the pKa values are very similar, the curves are practically overlapped. It is noteworthy that the formation of charged species begins at a pH of approximately 3 and reaches its maximum fraction at pH 7, which justifies the evaluation of solutions presenting pH values between 3 and 7. A low pH value, such as pH 3, was considered, despite the speciation diagram indicating that the species are mostly protonated under these conditions, as acidogenic fermentation processes are typically carried out in environments with pH values starting at this level [18]. Additionally, the dynamic transport of ions across the membranes during electrodialysis causes significant pH changes at the membrane/solution interface and in the bulk solution [21,22]. As a result, the initial pH of the feed solution is unlikely to remain constant throughout the process. This approach allows for evaluating electrodialysis performance under conditions in which the species are protonated, which is relevant for real-world applications with fluctuating pH.

3.1. Chronopotentiometry

The ChPs obtained for the Ralex, Fumasep, and PC200D membranes using feed solutions at the three studied pH values are shown in Fig. 2. pH values below 5 were not considered in the chronopotentiometric study because preliminary tests (not shown) indicated that the curves were very similar due to the low fraction of charged species. Fig. 2 shows the curves obtained under representative applied current densities, while the curves for all investigated current densities can be found in Figs. S3-S5 of the Supplementary Material.

As expected, the E_m of the curves obtained under low current densities with all membranes remained constant, due to the dominance of transport of VFAs by diffusion/migration. The pH increase of the feed solution from 5 to 7 did not affect the behavior of the ChPs of the Ralex membrane significantly (Fig. 2a-c). The curves obtained at the highest current densities exhibited intense oscillations, which may be associated either with the occurrence of electroconvection or, more likely, a

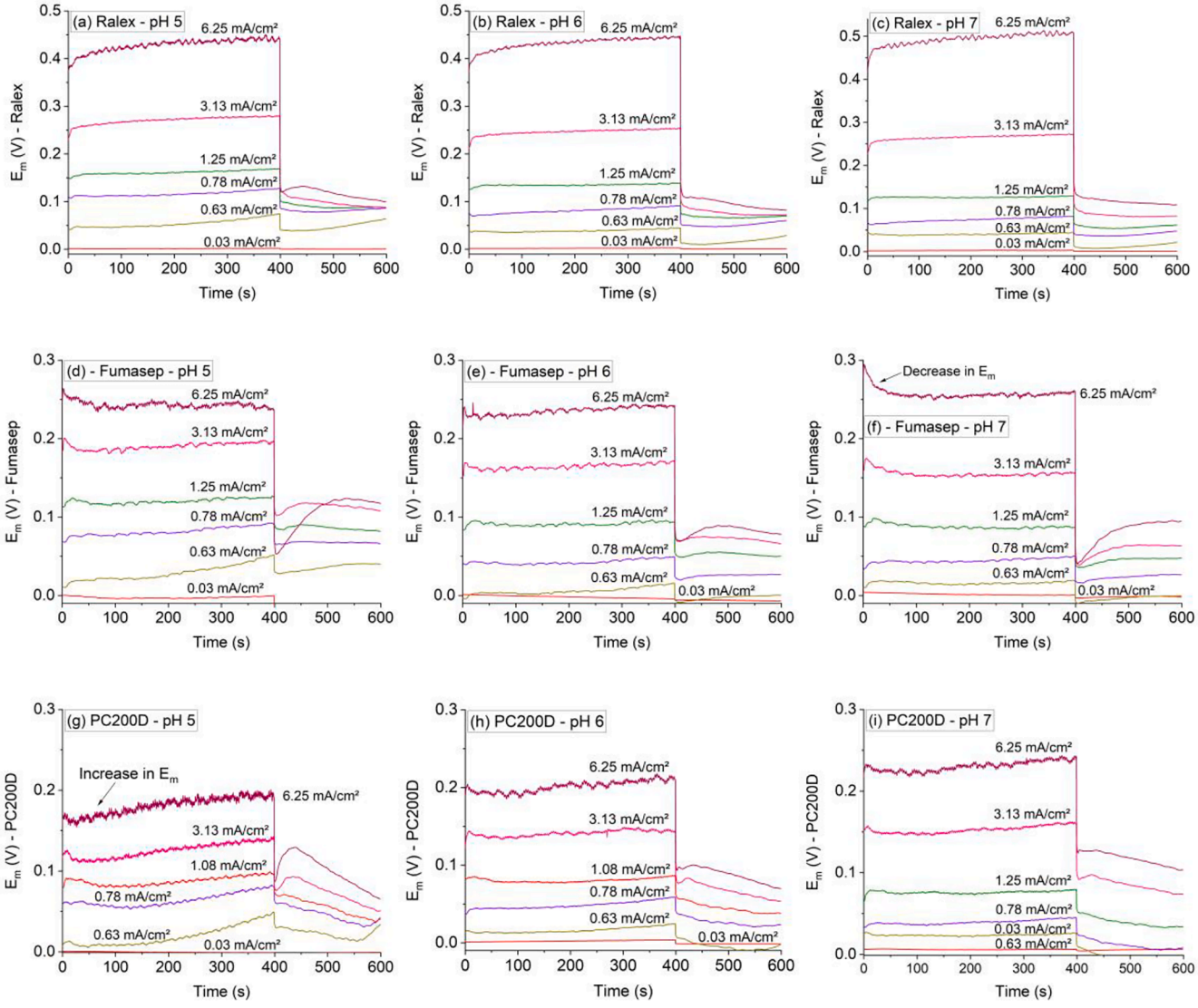

Fig. 2. ChPs obtained with the (a-c) Ralex, (d-f) Fumasep and (g-i) PC200D membrane and feed solution at pH 5, 6 and 7.

turbulized flow of the solutions caused by the spacers present since the oscillations have been verified for all AEMs shown in Fig. 2 [10]. Furthermore, for the Fumasep and PC200D membranes, oscillations were observed even in curves that indicated intense water dissociation occurrence, although electroconvection and water dissociation being competitive phenomena, which indicates that it is more likely that oscillations are due to solution turbulence. Although the curves for the Ralex did not indicate the occurrence of water dissociation at the membrane surface at any pH value, the relaxation section exhibited an atypical behavior for all membranes as E_m did not reach zero, especially after applying the highest current densities. This may have occurred due to the concentration gradients throughout the experiments, as ion transfer through the membranes under each current pulse altered the solution conditions.

The Fumasep curves obtained at the highest current densities also exhibited intense oscillations, which may be related to the solution turbulence, as discussed for the Ralex. A rapid increase in E_m at the beginning of the curve, when the current was applied, followed by a decrease was also observed (peak indicated in Fig. 2f). This is a typical behavior indicative of water dissociation at the membrane surface, as the H^+ and OH^- ions formed in the reaction increase the conductivity at the membrane/solution interface, thereby decreasing the electrical resistance and, consequently, the E_m [23]. This was more pronounced at pH 7 and can be explained by the fact that OH^- ions inhibit electroconvection, as they are transported via the Grotthuss mechanism without causing fluid movement [15,24]. As electroconvection and water dissociation are competing phenomena, water dissociation was enhanced at this condition. Besides, it is known that quaternary ammonium groups are converted into tertiary amines under current application, which intensifies water dissociation [25,26]. These results are consistent with the pH profiles of the bulk solutions over time, which is shown in Section 3.2.1.

Another possible reason for the E_m peak shown in Fig. 2d-f is the change in the species exchanged at the membrane's fixed charge when the membrane system shifted from the relaxed condition to the current application condition. In this case, the chemical equilibrium at the membrane surface was altered (increasing E_m), and then the quasi-steady state was reached (quasi-constant E_m).

The relaxation section also showed unexpected behavior. In most cases, a rapid drop of E_m as soon as the current application was interrupted was observed, followed by an increase, and then a subsequent decrease. This behavior may be attributed to the recombination of deprotonated VFAs with protons retained at the diluted solution/AEM membrane interface and was predominantly observed with the Fumasep and PC200D membranes due to the higher intensity of water dissociation occurring at these membranes.

The PC200D curves were similar for all pH values. When the highest current densities were applied, E_m showed a peak followed by a continuous increase over time, particularly with the solution at pH 5 (indicated in Fig. 2g). This is related to the development of concentration polarization and intense water dissociation occurrence at the membrane, forming H^+ at its diluted (feed) side. In this case, the retention of protons at the membrane due to their Donnan exclusion reduces the pH at its surface, thus altering the chemical equilibrium of the VFAs. As the pKa of the VFAs is approximately 4.8, the pH reduction led to the formation of uncharged species that increased the membrane resistance (see Fig. S2), causing the continuous increase in potential drop. This effect was not as pronounced at the highest pH (pH 7) due to the higher OH^- concentration, which prevented the achievement of pH values below 4.8 at the membrane surface. It is therefore recommended that the feed solution presents a pH of 6 or higher with the PC200D to avoid an increase in resistance. It is worth mentioning that this behavior was observed only with the PC200D membrane due to the presence of tertiary amines in its functional groups, which promote intense water dissociation and consequently alter the pH at the membrane surface.

3.1.1. Current-voltage curves

Fig. 3 shows the CVCs obtained for the Ralex, Fumasep and PC200D with the feed solution at initial pH values of 5, 6 and 7, and Table 1 presents the results of i_{lim}, R_{ohm}, and R_3 obtained from the curves.

The CVCs presented the typical shape with three well-defined regions (indicated in Fig. 3a): the quasi-ohmic (region 1), plateau (region 2), and overlimiting region (region 3) [27]. According to Table 1, the i_{lim} values of the membranes were relatively similar, whereas R_{ohm} and mainly R_3 showed variations presenting the following order: Ralex > Fumasep > PC200D. The highest resistance values obtained for Ralex were expected due to its heterogeneity and higher thickness, whereas the lowest ones obtained for PC200D may be due to its lower thickness [23]. The greater variations for R_3 than R_{ohm} among the membranes indicate that their structural differences affect their electrical resistance more intensely under overlimiting mechanisms (R_3) than under diffusion/migration (R_{ohm}). In this case, the heterogeneity of the membranes and the ability of their fixed charges to dissociate water were factors that contributed to amplifying the differences in the overlimiting current region ($i > i_{lim}$), which was not as relevant in the quasi-ohmic region due to the similar diffusion boundary layer for the three membranes.

Lastly, according to the LSV curve of the ED stack (Fig. S6 of the Supplementary Material), the current density of the ED system under application of 2.35 V with the feed solution at pH 6 was approximately 0.98 mA/cm^2. As the limiting current densities of the membrane/solution systems were approximately 0.6 mA/cm^2 with the solution at pH 6 (Table 1), the membrane systems operated in overlimiting regime, which means they were strongly influenced by water dissociation and/or electroconvection.

3.2. Electrodialysis

3.2.1. ED performance

Figs. 4 to 6 present the results of PE% of each VFA obtained with the Ralex, Fumasep and PC200D membranes, respectively, using feed solutions at initial pH values from 3 to 7. Figs. S7 to S9 show the same results plotted distinctly: each figure presents the PE% results obtained for the four VFAs using a feed solution at a given pH condition.

For the Ralex membrane (Fig. 4), the increase in pH enhanced the PE % of VFAs, particularly from 3 and 4 to 5, which can be explained by the pKa value of VFAs being approximately 4.8. In this case, VFAs were partially protonated at pH levels below 5, which hindered their transfer through the AEM. The transfer of VFAs, even at pH values lower than their pKa, occurred due to the presence of a small fraction of charged VFAs, as shown in Figure S2. The increase in pH from 5 to 7 did not significantly affect the PE% values.

For the Fumasep membrane (Fig. 5), the curves at pH 3 and 4 were nearly overlapping, indicating that the flux of each VFA within this pH range was identical. The increase in pH to 5 enhanced the PE%, as the VFAs became charged. However, increasing the pH from 5 to 6 or 7 caused a slight reduction in PE% of all VFAs, which can be explained by the competition between VFAs and OH^- species, especially those generated in the water dissociation reaction (Fig. 2). Therefore, for the Fumasep membrane, it is recommended that the feed solution presents an initial pH of 5 if the goal of electrodialysis is to recover all VFAs simultaneously in the same receiver solution, without considering their selective recovery.

The curves obtained for the PC200D showed distinct behaviors from the other membranes. At pH values of 3 and 4, the curves for each VFA were nearly overlapping, similar to what was observed for the Fumasep membrane and unlike what was observed for the Ralex. On the other hand, the increase in pH from 4 to 7 considerably enhanced the PE% of the VFAs with the PC200D, which was more pronounced for smaller VFAs (compare acetic acid with valeric acid). Thus, the PE% of VFAs obtained with PC200D was strongly influenced by the initial pH of the feed solution. This may be related to the presence of tertiary amines in its fixed groups, which intensified the occurrence of water dissociation

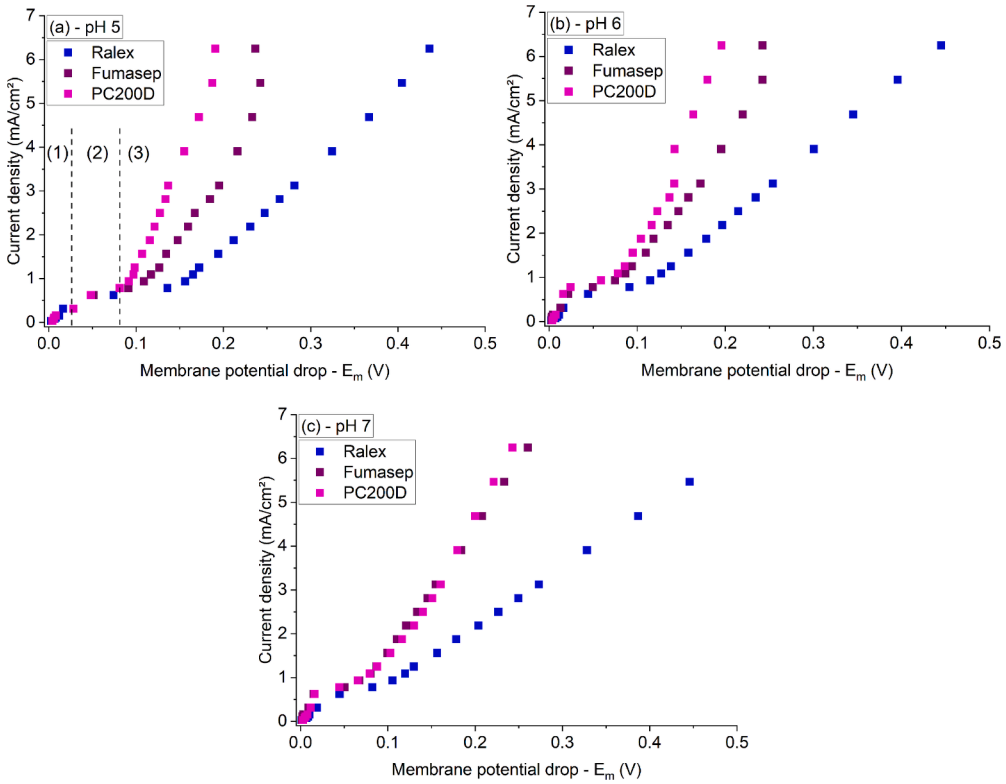

Fig. 3. CVCs for the Ralex, Fumasep and PC200D obtained with the feed solution at initial pH values of (a) 5, (b) 6 and (c) 7.

Table 1
Values of i_{lim} , R_{ohm} and R_3 obtained from the CVCs for the Ralex, Fumasep and PC200D membranes with the feed solution at initial pH values of 5, 6 and 7.

	Ralex	Fumasep	PC200D
		pH 5	
i_{lim} (mA/cm^2)	0.32	0.25	0.21
R_{ohm} (Ω·cm^2)	50	32	32
R_3 (Ω·cm^2)	53	33	19
		pH 6	
i_{lim} (mA/cm^2)	0.58	0.61	0.62
R_{ohm} (Ω·cm^2)	49	35	35
R_3 (Ω·cm^2)	61	34	22
		pH 7	
i_{lim} (mA/cm^2)	0.59	0.63	0.70
R_{ohm} (Ω·cm^2)	61	36	40
R_3 (Ω·cm^2)	75	34	29

especially with feed solution at greater pH values, forming H^+ and OH^- ions that increased the conductivity and consequently reduced the resistance of the membrane/electrolyte system. The lower resistance and transfer of OH^- ions may have altered the transport of each of the VFAs as a function of their size. The intense water dissociation occurrence at the PC200D is in accordance with the chronopotentiometric curves (Fig. 2g–i) and pH profiles vs. time, which will be shown below.

The pH profile vs. time of the feed and receiver solutions throughout the ED experiments is shown in Fig. 7. The figure presents the pH profiles obtained using the (a,d) Ralex, (b,e) Fumasep, and (c,f) PC200D membranes.

The feed solution curves exhibited similar behaviors for the three membranes. On the other hand, the receiver solution curves differed considerably.

For the Ralex, a reduction of the receiver pH was observed in all cases, which can be explained by the transfer of VFAs from the feed solution. For the Fumasep and mainly PC200D, a reduction of the pH of the receiver solution was observed with the feed solution at initial pH values of 3 and 4, which can be explained by the transfer of a small fraction of charged VFAs by electromigration or neutral VFAs by diffusion from the feed (Figure S2). For the ED conducted with feed solutions at initial pH values of 5, 6 or 7, the receiver solution showed a constant or increasing behavior. This can be explained by the intense occurrence of water dissociation at the diluted (feed) side of the Fumasep and PC200D membranes, as verified in the ChPs (Fig. 2d–f and g–i, respectively), and the consequent formation of OH^- ions. In this case, both OH^- and VFAs were simultaneously transferred to the concentrated compartment, maintaining the pH of the receiver solution relatively constant. It is worth mentioning that, although water dissociation occurs more intensely at AEMs [28], the pH of the solutions may have been affected by the occurrence of this phenomenon at the CEMs (Ralex CMH-PES) present at both extremities of the electrodialysis cell, generating H^+ and OH^- ions in the feed and receiver solutions. Moreover, the protons generated at the anode may have also affected the pH of the receiver solution, as they migrated through the CEM toward the cathode. In this case, as all experiments were conducted with the same CEM and under the same voltage, the effect of the protons generated at the anode should have been similar in all evaluations shown herein. Lastly, the dissociation and recombination of VFAs during their transfer through the AEM expectedly influenced the pH of both feed and receiver solutions. This occurred because the feed was acidified by dissociation of the VFAs at the solution/membrane interface contacting the feed solution prior to being transferred through the membrane, while the receiver solution was alkalinized by the recombination of VFAs with protons present in that solution.

As shown in Figs. S7 to S9, the general order of PE% obtained for the acids was acetic > propionic > butyric > valeric, which can be explained by their molecular sizes and diffusion coefficients (values at infinite dilution of $1.089{\cdot}10^{-5}$ cm^2/s, $0.953{\cdot}10^{-5}$ cm^2/s, $0.868{\cdot}10^{-5}$ cm^2/s, and $0.593{\cdot}10^{-5}$ cm^2/s, respectively [29,30]).

To facilitate the evaluation of the selective separation of VFAs, the ratios of the PE% for the following VFAs were calculated: $PE_{Ac}/(PE_{But} + PE_{Val})$, $PE_{Prop}/(PE_{But} + PE_{Val})$, $(PE_{Ac} + PE_{Prop})/(PE_{But} + PE_{Val})$, and

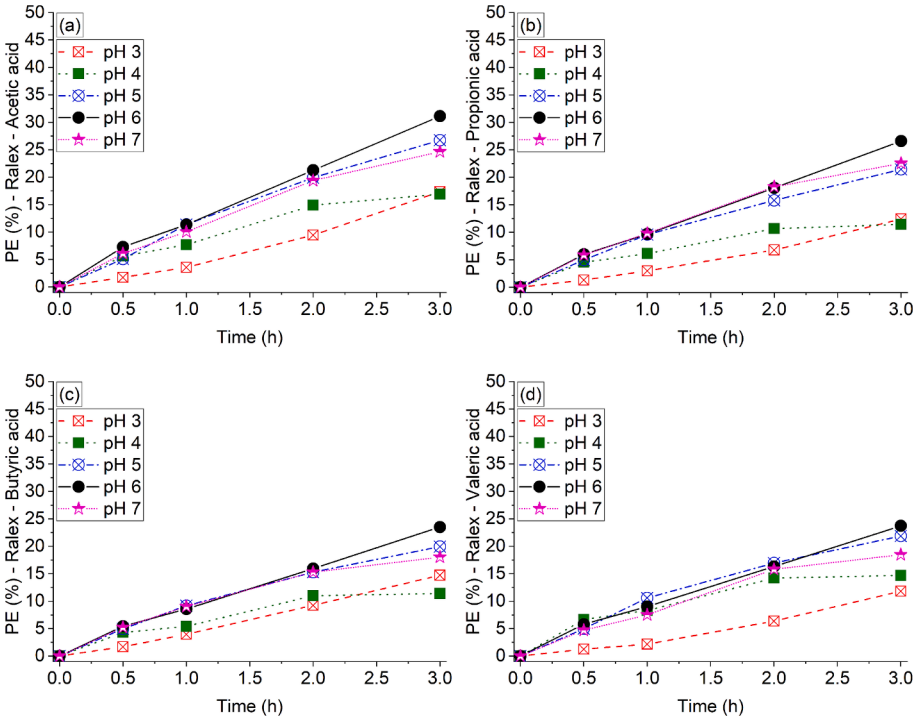

Fig. 4. PE% of (a) acetic, (b) propionic, (c) butyric and (d) valeric acids obtained with the Ralex membrane.

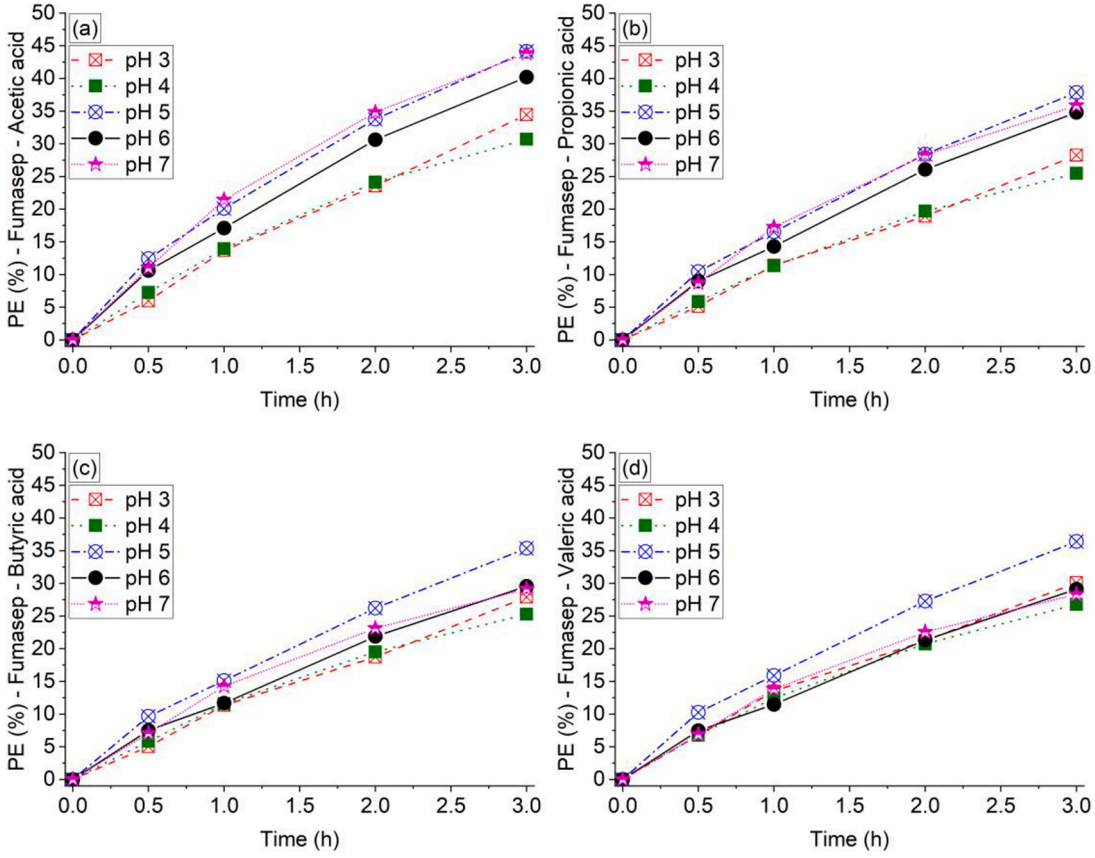

Fig. 5. PE% of (a) acetic, (b) propionic, (c) butyric and (d) valeric acids obtained with the Fumasep membrane.

$PEAc/PE_{Val}$. The results are presented in Table 2.

As shown in Table 2, the membranes led to different VFAs ratios as a function of initial feed pH. Regarding the $PE_{Ac}/(PE_{But} + PE_{Val})$ ratio, the Ralex membrane exhibited relatively constant values as the initial feed pH increased from 3 to 7, while the ratio for Fumasep membrane showed a slight increase from 0.6 to 0.8. The PC200D membrane exhibited a

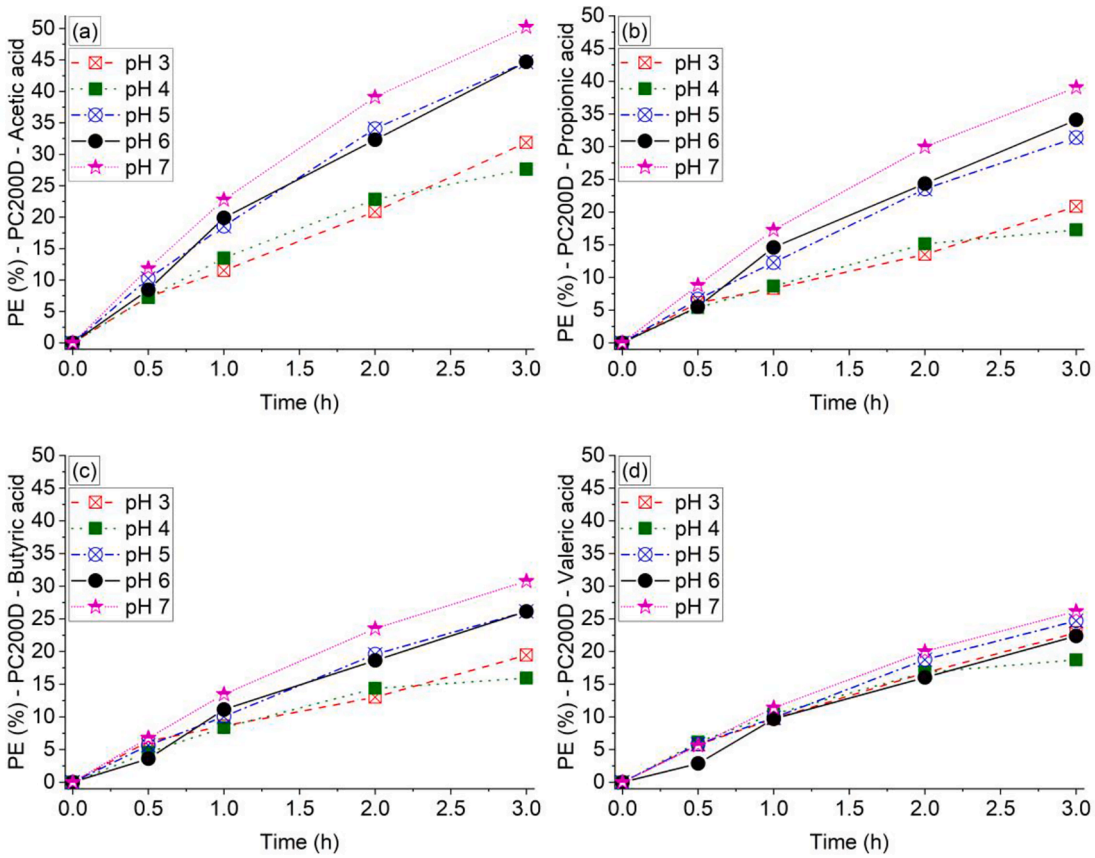

Fig. 6. PE% of (a) acetic, (b) propionic, (c) butyric and (d) valeric acids obtained with the PC200D membrane.

more pronounced ratio increase, ranging from approximately 0.6 to 1.0. This indicates that the separation of acetic acid from butyric and valeric acids was increased significantly with increasing pH only when using the PC200D membrane.

The $PE_{Prop}/(PE_{But} + PE_{Val})$ ratios obtained with all membranes were lower than the $PE_{Ac}/(PE_{But} + PE_{Val})$ ratios due to the greater size similarity of propionic, butyric and valeric compared to acetic, butyric and valeric acids. In general, the $PE_{Prop}/(PE_{But} + PE_{Val})$ ratios exhibited similar behavior: a slight increase for the Ralex and Fumasep membranes (ranging from 0.4 to 0.6) and the PC200D (ranging from 0.5 to 0.7). These results indicate that increasing the initial feed pH has a smaller effect on the separation of propionic acid from butyric and valeric acids compared to the separation of acetic from butyric and valeric acids.

The $(PE_{Ac} + PE_{Prop})/(PE_{But} + PE_{Val})$ ratios, which are the most relevant parameter as the aim of the study is to assess the separation of acetic and propionic acids from butyric and valeric acids, showed significant differences among the membranes. For the Ralex, the ratio increased from 1.0 to 1.2 as the pH rose from 3 to 7. For the Fumasep, the increase was from 1.0 to 1.4, and for the PC200D, it ranged from 1.1 to 1.6. This indicates that it was possible to achieve more than 50 % fractionation of the acetic + propionic and butyric + valeric acid pairs using the PC200D membrane only at pH values of 6 and 7.

Finally, the PE_{Ac}/PE_{Val} ratios, which reflect the separation of the smallest and largest VFAs evaluated here, showed no clear trend of increase or decrease with increasing initial feed pH for the Ralex membrane. In contrast, these ratios increased with the Fumasep membrane (from 1.0 to 1.5) and especially with the PC200D membrane (from 1.2 to 2.0).

The general order of the VFAs ratios was PC200D > Fumasep > Ralex at all pHs. For the Fumasep and mainly PC200D, the greater the pH, the greater the ratios, especially the $(PE_{Ac} + PE_{Prop})/(PE_{But} + PE_{Val})$ one, which means that the transfer of smaller ions (acetic and propionic acids) and the retention of bigger ions (butyric and valeric acids) were intensified. This may be explained by the greater intensity of water dissociation at high pH conditions, as indicated by the ChPs of the membranes and the pH profiles over time. In this case, the OH^- ions formed in the water dissociation reaction competed with the VFAs to be transferred, thus hindering the transfer of VFAs having a bigger size. Thus, smaller VFAs tend to be transferred through the membrane together with the formed OH^- ions, while bigger VFAs tend to be retained more intensely at the membrane. The low selectivity of VFA transport using the Ralex membrane may be explained by its high electric resistance when operated at overlimiting condition (R_3 in Table 1). In this case, R_3 remained high throughout the electrodialysis process, as intense water dissociation did not occur at this membrane, and therefore, OH^- ions were not significantly formed.

Lastly, separating VFAs into two solutions, one enriched with acetic and propionic acids, and the other enriched with butyric and valeric acids, offers economic and operational advantages in PHA production by MMCs. Specifically, studies have shown that PHA-accumulating MMCs preferentially consume longer-chain VFAs (butyric and valeric acids) for PHA synthesis before utilizing shorter-chain VFAs (acetic and propionic acids) [31], as from an energetic standpoint, this is more advantageous for the cells. Therefore, providing these longer-chain VFAs during PHA synthesis benefits the PHA accumulation stage. ED enables the partial fractionation of longer-chain VFAs from shorter-chain VFAs, and consequently offers the potential to manipulate the monomeric composition of the copolymer scl-PHA, as the ratio of 3HB to 3HV depends on the availability of their precursors.

3.2.2. Mass balances of VFAs

The results of mass balances for VFAs are presented in Table S2 of the Supplementary Material. Note that in some cases, the values did not

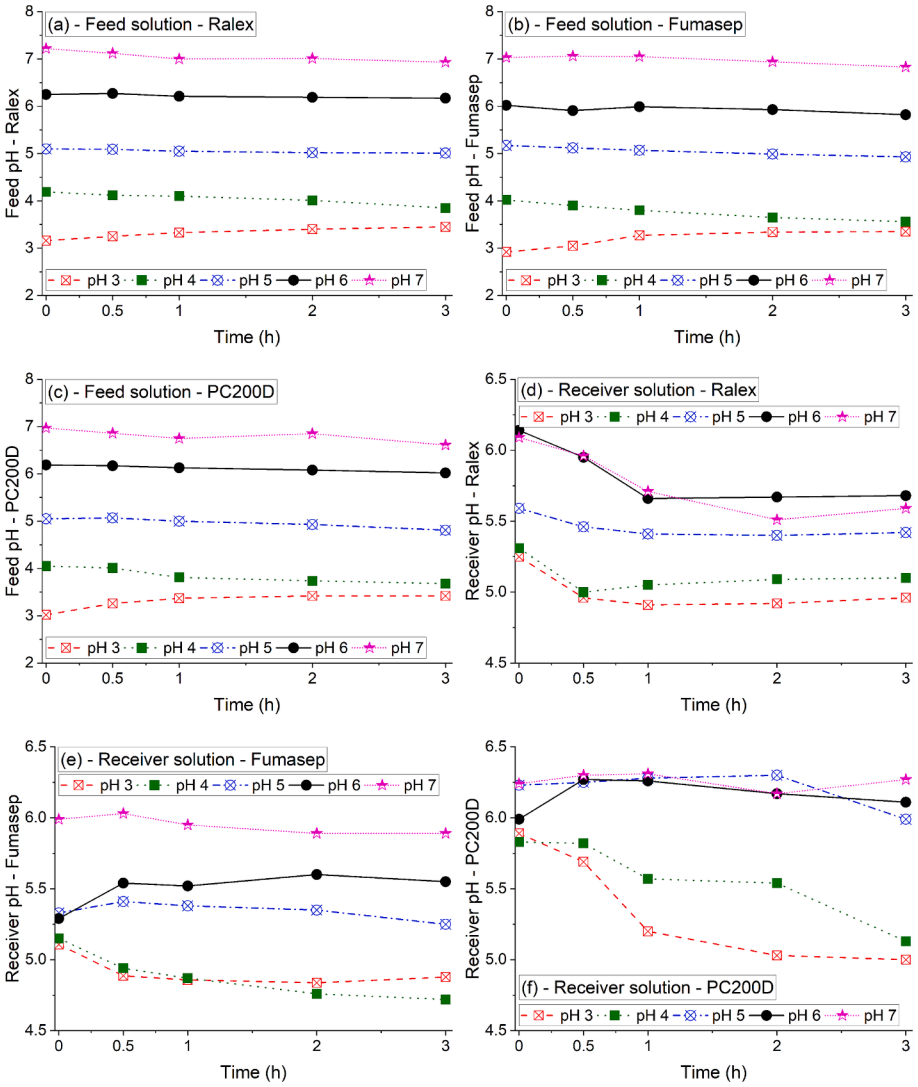

Fig. 7. pH vs. time profile for the solutions from the ED tests conducted with the (a,d) Ralex, (b, e) Fumasep, and (c,f) PC200D membranes.

reach 100 %, which suggests that the VFAs were retained in the membranes due to the sorption phenomenon. This occurred more intensely at the Ralex membrane using the feed solution with an initial pH value of 5 or 6, since the mass balance values were considerably lower than 100 %. The lower sorption intensity at pH 3 and pH 4 with the Ralex can be explained by the smaller fraction of charged species in solution, which reduced the attraction between VFAs and the fixed charges of the membrane. On the other hand, the lower sorption intensity at pH 7 can be attributed to the high concentration of OH^-, which desorbed the VFAs from the functional groups. No significant sorption was observed for the Fumasep membrane at any pH condition. For the PC200D membrane, sorption occurred only for the valeric acid at lower pH values (pH 3 and pH 4), which can be explained by its larger size and higher degree of hydrophobicity, as the more hydrophobic a solute is, the greater its sorption onto the membrane [32,33]. In this case, sorption occurred mainly by diffusion due to the lack of charge on the VFA. This is in agreement with the recent works published by Aghapour Aktij et al. [34] and Ramos-Suarez et al. [35], who found that VFAs are primarily adsorbed through diffusion in ion-exchange materials containing tertiary amines when they are in their protonated state due to hydrophobic interactions. Lastly, the lower VFAs sorption observed for the Fumasep and PC200D membranes compared to that of the Ralex membrane can be explained by their lower thickness (Table S1) [36,37].

4. Conclusions

The results showed that the initial feed pH plays an important role in the selective recovery of VFAs from fermented solutions by electrodialysis, especially with the PC200D membrane. Increasing the initial feed pH with this membrane primarily impacted the percent extraction of smaller VFAs, such as acetic and propionic acids. On the other hand, the PE% of larger acids, such as butyric and valeric, was practically unaffected. These results indicate that, for the selective separation of VFAs using the PC200D, an initial feed solution pH of 7 is recommended, as it improves the PE% ratios of the VFA pairs. For the ED operated under this condition, $(PE_{Ac} + PE_{Prop})/(PE_{But} + PE_{Val})$ and PE_{Ac}/PE_{Val} ratios of 1.6 and 2.0, respectively, were obtained. Conversely, the Ralex membrane exhibited minimal sensitivity to changes in the initial feed pH, whereas for the Fumasep membrane an increase in the initial feed pH led to a reduction in percent extraction values but resulted in a slight increase in fractionation degrees. The higher degree of VFA separation achieved with PC200D may be explained by the presence of tertiary amines in its functional groups, which intensified the occurrence of water dissociation at the membrane, and its low resistance.

In the context of PHA production, the results demonstrate the feasibility of producing fermented solutions with higher concentrations of butyric and valeric acids, compared to smaller VFAs like acetic and propionic acids, while also contributing to the fractionating 3HB and

Table 2
PE% ratios of PE_{Ac} /(PE_{But} + PE_{Val}), PE_{Prop} /(PE_{But} + PE_{Val}), (PE_{Ac} + PE_{Prop})/(PE_{But} + PE_{Val}), and PE_{Ac} /PE_{Val} for the ED tests.

		$PE_{Ac}/(PE_{But}+PE_{Val})$			$PE_{Prop}/(PE_{But}+PE_{Val})$			$(PE_{Ac}+PE_{Prop})/(PE_{But}+PE_{Val})$			PE_{Ac}/PE_{Val}		
pH	Time (h)	Ralex	Fumasep	PC 200D	Ralex	Fumasep	PC 200D	Ralex	Fumasep	PC 200D	Ralex	Fumasep	PC 200D
3	0.5	0.64	0.51	0.61	0.44	0.44	0.51	1.08	0.94	1.12	1.51	0.88	1.27
	1	0.55	0.55	0.63	0.48	0.46	0.45	1.03	1.01	1.08	1.55	1.01	1.18
	2	0.61	0.59	0.70	0.43	0.47	0.45	1.04	1.06	1.16	1.48	1.11	1.25
	3	0.65	0.59	0.75	0.47	0.49	0.49	1.12	1.08	1.25	1.47	1.14	1.39
4	0.5	0.51	0.58	0.68	0.41	0.46	0.50	0.93	1.04	1.18	0.84	1.07	1.18
	1	0.56	0.58	0.72	0.45	0.47	0.46	1.01	1.05	1.18	0.93	1.12	1.30
	2	0.59	0.60	0.73	0.42	0.49	0.49	1.01	1.09	1.22	1.05	1.16	1.36
	3	0.65	0.59	0.80	0.44	0.49	0.50	1.09	1.08	1.30	1.15	1.15	1.48
5	0.5	0.51	0.62	0.89	0.50	0.52	0.58	1.01	1.15	1.48	1.03	1.21	1.76
	1	0.58	0.65	0.93	0.48	0.53	0.62	1.06	1.18	1.55	1.08	1.26	1.88
	2	0.62	0.63	0.89	0.49	0.53	0.61	1.11	1.16	1.50	1.18	1.24	1.82
	3	0.64	0.61	0.88	0.51	0.53	0.62	1.15	1.14	1.50	1.22	1.21	1.81
6	0.5	0.65	0.71	1.30	0.53	0.60	0.85	1.18	1.31	2.15	1.25	1.42	2.94
	1	0.65	0.74	0.96	0.55	0.62	0.70	1.20	1.36	1.66	1.26	1.49	2.05
	2	0.66	0.71	0.93	0.56	0.60	0.70	1.22	1.31	1.63	1.30	1.44	2.02
	3	0.66	0.69	0.92	0.56	0.59	0.70	1.22	1.28	1.62	1.31	1.38	2.00
7	0.5	0.56	0.79	0.96	0.54	0.62	0.71	1.10	1.41	1.66	1.08	1.60	2.11
	1	0.54	0.76	0.92	0.53	0.62	0.69	1.06	1.38	1.61	1.04	1.55	2.00
	2	0.68	0.76	0.90	0.62	0.62	0.69	1.29	1.38	1.59	1.33	1.55	1.95
	3	0.62	0.76	0.88	0.59	0.62	0.69	1.21	1.39	1.57	1.23	1.55	1.92

*Colors considered for each range of VFA ratios:

Minimum	Maximum
0.4	0.649
0.65	0.8449
0.845	1.14
1.141	1.54
1.545	1.99
2.0	4.0

3HV precursor molecules for use during the PHA accumulation stage. This approach is anticipated to enhance PHA accumulation yields and enable better control over the monomer composition of the resulting PHA biopolymers.

Declaration of competing interest

The authors declare that they have no known competing financial interests or personal relationships that could have appeared to influence the work reported in this paper.

Acknowledgments

The authors gratefully acknowledge the financial support given by Universitat Politècnica de València and Ministerio de Universidades de España (Plan de Recuperación, Transformación y Resiliencia – financed by European Union - Next GenerationEU). This work was also financed by Fundação para a Ciência e a Tecnologia, I.P., Lisbon, Portugal in the scope of the SaltiPHA (PTDC/BTA-BTA/30902/2017), Laboratório Associado para a Química Verde - Tecnologias e Processos Limpos – LAQV (UIDB/50006/2020 and UIDP/50006/2020), Research Unit on Applied Molecular Biosciences – UCIBIO (UIDP/04378/2020 and UIDB/04378/2020), Associate Laboratory Institute for Health and Bio-economy - i4HB (LA/P/0140/2020).

Appendix A. Supplementary material

Supplementary data to this article can be found online at https://doi.org/10.1016/j.seppur.2025.132550.

Data availability

Data will be made available on request.

References

[1] J.B. Silva, J.R. Pereira, B.C. Marreiros, M.A.M. Reis, F. Freitas, Microbial production of medium-chain length polyhydroxyalkanoates, Process Biochem. 102 (2021) 393–407, https://doi.org/10.1016/j.procbio.2021.01.020.
[2] C. Kourmentza, J. Plácido, N. Venetsaneas, A. Burniol-Figols, C. Varrone, H. N. Gavala, M.A.M. Reis, Recent advances and challenges towards sustainable polyhydroxyalkanoate (PHA) production, Bioengineering 4 (2017) 55, https://doi.org/10.3390/bioengineering4020055.
[3] M. Carvalheira, B.C. Marreiros, M.A.M. Reis, Acids (VFAs) and bioplastic (PHA) recovery, Clean Energy Resource Recovery: Wastewater Treatment Plants as

Biorefineries 2 (2022) 245–254, https://doi.org/10.1016/B978-0-323-90178-9.00016-0.
[4] J.M. Dias, A. Oehmen, L.S. Serafim, P.C. Lemos, M.A. Reis, R. Oliveira, Metabolic modelling of polyhydroxyalkanoate copolymers production by mixed microbial cultures, BMC Syst. Biol. 2 (2008) 59, https://doi.org/10.1186/1752-0509-2-59.
[5] X.Z. Zhu, L.F. Wang, X.R. Pan, F. Zhang, M.S. Huang, W.W. Li, H.Q. Liu, Selective separation of volatile fatty acids, nitrogen and phosphorus from anaerobic acidogenic fermentation via forward osmosis membrane process, Chem. Eng. J. 453 (2023) 139871, https://doi.org/10.1016/j.cej.2022.139871.
[6] A.T. Giduthuri, B.K. Ahring, Current status and prospects of valorizing organic waste via arrested anaerobic digestion: production and separation of volatile fatty acids, Fermentation 9 (2023), https://doi.org/10.3390/fermentation9010013.
[7] K.S. Barros, M. Carvalheira, B.C. Marreiros, M.A.M. Reis, J.G. Crespo, V. Pérez-Herranz, S. Velizarov, Donnan dialysis for recovering ammonium from fermentation solutions rich in volatile fatty acids, Membranes (Basel) 13 (2023) 347, https://doi.org/10.3390/membranes13030347.
[8] K.S. Barros, B.C. Marreiros, M. Carvalheira, M.A.M. Reis, J.G. Crespo, V. Pérez-Herranz, S. Velizarov, Evaluation of fouling phenomena and cation-exchange membrane cleaning in Donnan dialysis for separation of ammonium from fermented solutions rich in volatile fatty acids, Sep. Purif. Technol. 356 (2025) 129834, https://doi.org/10.1016/j.seppur.2024.129834.
[9] R. Chalmers Brown, R. Tuffou, J. Massanet Nicolau, R. Dinsdale, A. Guwy, Overcoming nutrient loss during volatile fatty acid recovery from fermentation media by addition of electrodialysis to a polytetrafluoroethylene membrane stack, Bioresour. Technol. 301 (2020) 122543, https://doi.org/10.1016/j.biortech.2019.122543.
[10] K.S. Barros, B.C. Marreiros, M.A.M. Reis, J.G. Crespo, V. Pérez-Herranz, S. Velizarov, Recovery and fractionation of volatile fatty acids from fermented solutions by electrodialysis: electrochemical characterization of anion-exchange membranes, J. Environ. Chem. Eng. (2024) 114457, https://doi.org/10.1016/j.jece:2024.114457.
[11] A. Chandra, B. E, S. Chattopadhyay, A critical analysis on ion transport of organic acid mixture through an anion-exchange membrane during electrodialysis, Chem. Eng. Res. Des. 178 (2022) 13–24, https://doi.org/10.1016/j.cherd.2021.11.035.
[12] M.C. Martí-Calatayud, M. Ruiz-García, V. Pérez-Herranz, On the selective transport of mixtures of organic and inorganic anions through anion-exchange membranes: a case study about the separation of nitrates and citric acid by electrodialysis, Sep. Purif. Technol. 354 (2025), https://doi.org/10.1016/j.seppur.2024.128951.
[13] Y. Tanaka, Water dissociation reaction generated in an ion exchange membrane, 350 (2010) 347–360. doi: 10.1016/j.memsci.2010.01.010.
[14] F. Meng, S. Zhang, Y. Oh, Z. Zhou, H.S. Shin, S.R. Chae, Fouling in membrane bioreactors: an updated review, Water Res 114 (2017) 151–180, https://doi.org/10.1016/j.watres.2017.02.006.
[15] M.C. Martí-Calatayud, K.S. Barros, Concentration polarization in ion-exchange membranes, in: Current Trends and Future Developments on (bio-) Membranes, Elsevier, 2024, pp. 321–345, https://doi.org/10.1016/B978-0-323-88509-6.00002-2.
[16] A. Gorobchenko, O. Yurchenko, S. Mareev, C. Zhang, N. Pismenskaya, V. Nikonenko, Study of non-stationary phosphorus transport with phosphoric acid anions through an anion-exchange membrane by chronopotentiometry: experiments and modeling, J. Water Process Eng. 64 (2024), https://doi.org/10.1016/j.jwpe.2024.105711.
[17] J.-H. Choi, H.-J. Lee, S.-H. Moon, Effects of electrolytes on the transport phenomena in a cation-exchange membrane, J. Colloid Interf. Sci. 238 (2001) 188–195, https://doi.org/10.1006/jcis.2001.7510.
[18] H. Liu, J. Wang, X. Liu, B. Fu, J. Chen, H.Q. Yu, Acidogenic fermentation of proteinaceous sewage sludge: Effect of pH, Water Res. 46 (2012) 799–807, https://doi.org/10.1016/j.watres.2011.11.047.
[19] B.C. Fonseca, J. Bortolucci, T.M. da Silva, V.F. dos Passos, P.F. de Gouvêa, T. M. Dinamarco, V. Reginatto, Butyric acid as sole product from xylose fermentation by a non-solventogenic Clostridium beijerinckii strain under controlled pH and nutritional conditions, Bioresour. Technol. Rep. 10 (2020), https://doi.org/10.1016/j.biteb.2020.100426.
[20] Z.K. Jia, D.M. Du, Z.y. Zhou, A.G. Zhang, R.Y. Hou, Accurate pKa determinations for some organic acids using an extended cluster method, Chem. Phys. Lett. 439 (2007) 374–380, https://doi.org/10.1016/j.cplett.2007.03.092.
[21] N.D. Pismenskaya, O.A. Rybalkina, A.E. Kozmai, K.A. Tsygurina, E.D. Melnikova, V.V. Nikonenko, Generation of H^+ and OH^- ions in anion-exchange membrane/ampholyte-containing solution systems: a study using electrochemical impedance spectroscopy, J. Memb. Sci. 601 (2020) 117920, https://doi.org/10.1016/j.memsci.2020.117920.
[22] O.A. Rybalkina, M.V. Sharafan, V.V. Nikonenko, N.D. Pismenskaya, Two mechanisms of H^+/OH^- ion generation in anion-exchange membrane systems with polybasic acid salt solutions, J. Memb. Sci. 651 (2022) 120449, https://doi.org/10.1016/j.memsci.2022.120449.
[23] N. Pismenskaia, P. Sistat, P. Huguet, V. Nikonenko, G. Pourcelly, Chronopotentiometry applied to the study of ion transfer through anion exchange membranes, J. Memb. Sci. 228 (2004) 65–76, https://doi.org/10.1016/j.memsci.2003.09.012.
[24] R.A. Tufa, M.T. Tsehaye, W. Zhang, M. Aquino, S. Santoro, E. Curcio, Transport and Conductive Mechanisms in Anion Exchange Membranes, in: Alkaline anion exchange membranes for fuel cells, Wiley, 2024, pp. 125–142, https://doi.org/10.1002/9783527837588.ch6.
[25] V.I. Zabolotskii, R.K. Chermit, M.V. Sharafan, Mass transfer mechanism and chemical stability of strongly basic anion-exchange membranes under overlimiting current conditions, Russ. J. Electrochem. 50 (2014) 38–45, https://doi.org/10.1134/S102319351401011X.
[26] D.Y. Butylskii, V.A. Troitskiy, M.V. Sharafan, N.D. Pismenskaya, V.V. Nikonenko, Scaling-resistant anion-exchange membrane prepared by in situ modification with a bifunctional polymer containing quaternary amino groups, Desalination 537 (2022), https://doi.org/10.1016/j.desal.2022.115821.
[27] V.D. Titorova, S.A. Mareev, A.D. Gorobchenko, V.V. Gil, V.V. Nikonenko, K. G. Sabbatovskii, N.D. Pismenskaya, Effect of current-induced coion transfer on the shape of chronopotentiograms of cation-exchange membranes, J. Memb. Sci. (2021) 119036, https://doi.org/10.1016/j.memsci.2020.119036.
[28] K.S. Barros, A. Giacobbo, G.D. Agnol, S. Velizarov, V. Pérez-Herranz, A. M. Bernardes, Evaluation of mass transfer behaviour of sulfamethoxazole species at ion–exchange membranes by chronopotentiometry for electrodialytic processes, J. Electroanal. Chem. 931 (2023) 117214, https://doi.org/10.1016/j.jelechem.2023.117214.
[29] D.R. Lide, Handbook of Chemistry and Physics, CRC Press, New York, 1997.
[30] C.L. Yaws, Diffusion Coefficient in Water – Organic Compounds, in: Transport properties of chemicals and hydrocarbons, Elsevier, 2009, pp. 502–593, https://doi.org/10.1016/B978-0-8155-2039-9.50017-X.
[31] J.M. Carvalho, B.C. Marreiros, M.A.M. Reis, Polyhydroxyalkanoates production by mixed microbial culture under high salinity, Sustainability (Switzerland) 14 (2022) 1–15, https://doi.org/10.3390/su14031346.
[32] Z. Li, W. Qin, Y. Dai, Liquid-liquid equilibria of acetic, propionic, butyric, and valeric acids with trioctylamine as extractant, J. Chem. Eng. Data 47 (2002) 843–848, https://doi.org/10.1021/je015526t.
[33] H.M. Haflich, J.W. Singleton, O. Coronell, Relative contributions of mobility and partitioning to volatile fatty acid flux during electrodialysis, J. Memb. Sci. 711 (2024), https://doi.org/10.1016/j.memsci.2024.123204.
[34] S. Aghapour Aktij, A. Zirehpour, A. Mollahosseini, M.J. Taherzadeh, A. Tiraferri, A. Rahimpour, Feasibility of membrane processes for the recovery and purification of bio-based volatile fatty acids: a comprehensive review, J. Ind. Eng. Chem. 81 (2020) 24–40, https://doi.org/10.1016/j.jiec.2019.09.009.
[35] M. Ramos-Suarez, Y. Zhang, V. Outram, Current perspectives on acidogenic fermentation to produce volatile fatty acids from waste, Rev. Environ. Sci. Biotechnol. 20 (2021) 439–478, https://doi.org/10.1007/s11157-021-09566-0.
[36] R. Epsztein, E. Shaulsky, M. Qin, M. Elimelech, Activation behavior for ion permeation in ion-exchange membranes: role of ion dehydration in selective transport, J. Memb. Sci. 580 (2019) 316–326, https://doi.org/10.1016/j.memsci.2019.02.009.
[37] M.A. Izquierdo-Gil, V.M. Barragán, J.P.G. Villaluenga, M.P. Godino, Water uptake and salt transport through Nafion cation-exchange membranes with different thicknesses, Chem. Eng. Sci. 72 (2012) 1–9, https://doi.org/10.1016/j.ces.2011.12.040.